NASA/TM—2007–214959

Application of Simulated Reactivity Feedback in Nonnuclear Testing of a Direct-Drive Gas-Cooled Reactor

S.M. Bragg-Sitton and K.L. Webster
Marshall Space Flight Center, Marshall Space Flight Center, Alabama

June 2007

The NASA STI Program…in Profile

Since its founding, NASA has been dedicated to the advancement of aeronautics and space science. The NASA Scientific and Technical Information (STI) Program Office plays a key part in helping NASA maintain this important role.

The NASA STI program operates under the auspices of the Agency Chief Information Officer. It collects, organizes, provides for archiving, and disseminates NASA's STI. The NASA STI program provides access to the NASA Aeronautics and Space Database and its public interface, the NASA Technical Report Server, thus providing one of the largest collections of aeronautical and space science STI in the world. Results are published in both non-NASA channels and by NASA in the NASA STI Report Series, which includes the following report types:

- TECHNICAL PUBLICATION. Reports of completed research or a major significant phase of research that present the results of NASA programs and include extensive data or theoretical analysis. Includes compilations of significant scientific and technical data and information deemed to be of continuing reference value. NASA's counterpart of peer-reviewed formal professional papers but has less stringent limitations on manuscript length and extent of graphic presentations.

- TECHNICAL MEMORANDUM. Scientific and technical findings that are preliminary or of specialized interest, e.g., quick release reports, working papers, and bibliographies that contain minimal annotation. Does not contain extensive analysis.

- CONTRACTOR REPORT. Scientific and technical findings by NASA-sponsored contractors and grantees.

- CONFERENCE PUBLICATION. Collected papers from scientific and technical conferences, symposia, seminars, or other meetings sponsored or cosponsored by NASA.

- SPECIAL PUBLICATION. Scientific, technical, or historical information from NASA programs, projects, and missions, often concerned with subjects having substantial public interest.

- TECHNICAL TRANSLATION. English-language translations of foreign scientific and technical material pertinent to NASA's mission.

Specialized services also include creating custom thesauri, building customized databases, and organizing and publishing research results.

For more information about the NASA STI program, see the following:

- Access the NASA STI program home page at <http://www.sti.nasa.gov>

- E-mail your question via the Internet to <help@sti.nasa.gov>

- Fax your question to the NASA STI Help Desk at 301– 621–0134

- Phone the NASA STI Help Desk at 301– 621–0390

- Write to:
  NASA STI Help Desk
  NASA Center for AeroSpace Information
  7115 Standard Drive
  Hanover, MD 21076–1320

Application of Simulated Reactivity Feedback in Nonnuclear Testing of a Direct-Drive Gas-Cooled Reactor

S.M. Bragg-Sitton and K.L. Webster
Marshall Space Flight Center, Marshall Space Flight Center, Alabama

June 2007

TRADEMARKS

Trade names and trademarks are used in this report for identification only. This usage does not constitute an official endorsement, either expressed or implied, by the National Aeronautics and Space Administration.

TABLE OF CONTENTS

LIST OF FIGURES

LIST OF ACRONYMS

Ar	argon
API	application interface
AWG	American wire gauge
CCD	charge-coupled device
DDG	direct-drive gas
DVRT	differential variable reluctance transducer
EFF–TF	Early Flight Fission-Test Facility
He	helium
HeXe	helium-xenon
HP	heat pipe
HX`	heat exchanger
MSFC	Marshall Space Flight Center
Na	sodium
PCI	peripheral component interconnect
PKE	point kenetics equation
SAFE	Safe Affordable Fission Engine
TC	thermocouple
TCP–TP	transmission control protocol-internet protocol
TM	Technical Memorandum

UDP   user datagram protocol

UN   uranium nitride

VMIC   VME Microsystems International Corporation

Xe   xenon

NOMENCLATURE

A	heat transfer area (m^2)
C_i	delayed-neutron concentration, ith precursor group
C_p	specific heat of the coolant
$C_{p,struct}$	specific heat of the core structure
dL	measured core deflection, ultimately a function of temperature at any given time
F_s	data sample rate (s)
h_c	convective heat transfer coefficient (assumed constant)
k	effective neutron multiplication factor
$M_{coolant}$	mass of the coolant in the core (kg)
M_{struct}	mass of the core structure (kg)
$\dot{m}$	mass flow rate (assumed constant) (kg/s)
P	reactor thermal power (W)
P_{Rx}	reactor thermal power (W)
T	temperature (K)
T_{in}	coolant inlet temperature (K)
$T_{coolant,avg}$	average temperature of coolant in the core (K)
T_{out}	coolant exit temperature (K)
T_{struct}	average structural temperature (K)
t	time (s)
α_T	temperature coefficient of reactivity

β total delayed-neutron fraction (sum of all β_i)

β_i delayed-neutron fraction, ith precursor group

Λ prompt neutron generation time (s)

λ_i decay constant for the ith precursor group (s^{-1})

ρ reactivity

TECHNICAL MEMORANDUM

APPLICATION OF SIMULATED REACTIVITY FEEDBACK IN NONNUCLEAR TESTING OF A DIRECT-DRIVE GAS-COOLED REACTOR

1. INTRODUCTION

Nonnuclear testing can be used to evaluate the operation of an integrated nuclear system within a reasonable cost and schedule in order to provide valuable input to the overall system design. Various operational regimes can be studied in nonnuclear testing to validate thermal and thermal hydraulic codes, assess thermal hydraulic behavior, characterize stress/strain in the system during operation, and verify system integration processes. However, because the electrically heated core lacks neutrons, the dynamic neutronic response of the system cannot be fully simulated without the incorporation of additional system models.

In early 2005, dynamic testing was performed on the Safe Affordable Fission Engine (SAFE) 100a test article at the NASA Marshall Space Flight Center (MSFC) Early Flight Fission Test Facility (EFF–TF). The SAFE–100a is a resistively heated, stainless steel heat pipe (HP) reactor core segment coupled to a prototypic gas-flow heat exchanger (HX). Core power transients that were simulated in the electrically heated system tests were controlled by a point kinetics model with reactivity feedback based on a bulk temperature reactivity feedback coefficient and core average temperature. This type of nonnuclear test is expected to provide a reasonable approximation of reactor transient behavior because reactivity feedback is very simple in a compact fast spectrum reactor (simple, negative, and relatively monotonic temperature feedback, caused mostly by thermal expansion) and calculations show that no significant reactivity effects are associated with fluid in the HP (the worth of the entire inventory of sodium (Na) in the core is much less than one dollar, so fluid movement and temperature changes will cause very minor effects). In previous SAFE–100 tests, the point kinetics model was based on core thermal expansion via deflection measurements.[1] These tests demonstrated that core deflection was a strong function of how the SAFE–100 modules were fabricated and assembled, in terms of straightness, gaps, and other tolerances. Both the SAFE–100 and 100a were constructed from individual modules that nested together to form a core rather than being constructed from a monolithic block. To remove the added variable of SAFE–100a expansion with varying temperature, as compared to a different concept, it was decided to use a temperature-based feedback model, based on several thermocouples (TCs) placed throughout the core. The bulk core temperature feedback coefficient for most reactors of this class is on the order of –0.1 to –0.2 cents per degree Kelvin.

The test matrix applied in SAFE–100a testing included changes in coolant flow rate to simulate system load variations and step reactivity insertions and decreases. The system responded as expected for all induced transients—increased/decreased coolant flow rate with reactivity feedback, increased/decreased coolant flow rate without reactivity feedback (done for comparison), and positive/negative reactivity insertion. Expected implies that the transient response was typical of any simple reactor, whether it be cooled by a pumped fluid (gas or liquid metal), or by HPs. Figure 1 shows the system response to a series of transients in which the system load was increased several times, represented by mass-flow increase through the HX, followed by a step reactivity insertion of $0.06. An in-depth discussion of the SAFE–100a system response can be found in reference 2.
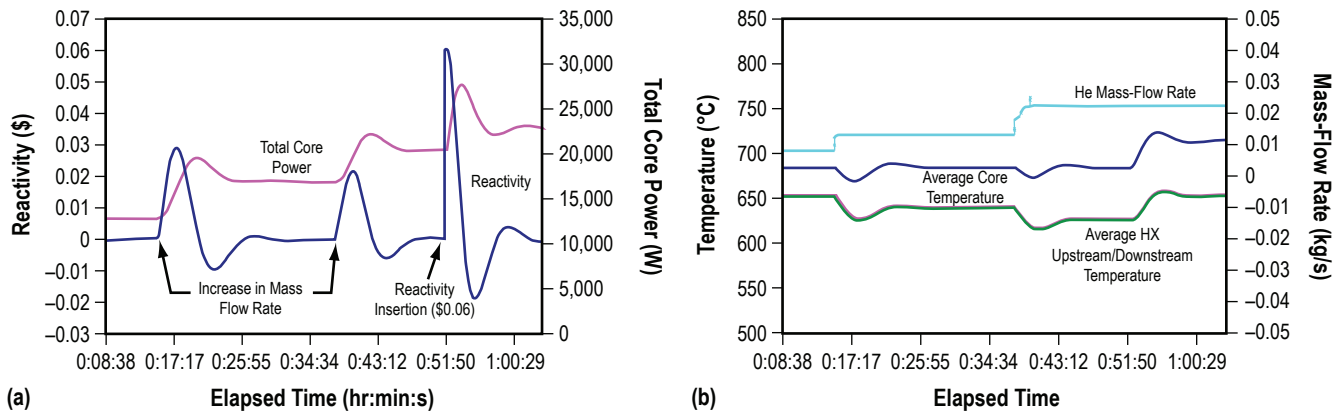

Figure 1. Dynamic system testing of the SAFE–100a with simulated reactivity feedback:
(a) Core thermal power and calculated reactivity and (b) HX mass-flow rate,
average core temperature, and average HP temperatures upstream and
downstream of the HX.

During the applied transients, the HPs appear to act as very good conductors with relatively little thermal inertia, such that system response would be expected to be very similar in a reactor design in which gas directly removes power from the core, as in a direct-drive gas (DDG) cooled reactor that does not incorporate an intermediate HX. The time scale of the transient is dictated mostly by the thermal inertia of the core, with a smaller extent being dictated by the HPs and HX for the SAFE–100a. In each transient applied to the SAFE–100a, the peaks and valleys of the power and temperature occurred within 3–5 min after transient initiation, followed by modest oscillations until the system stabilized at a new steady state condition approximately 20–30 min after the transient was initiated. The magnitude of power and temperature overshoots were also modest; ≈15 K temperature overshoot for a $0.10 reactivity insertion, although the magnitude of overshoot is not of great meaning because the SAFE–100a is a low-power density core with nonprototypic thermal inertia.

Similar dynamic test methodology is planned for application with the electrically heated, DDG test article currently undergoing testing at MSFC. Designed by engineers at Sandia National Laboratory and the Los Alamos National Laboratory, the DDG was previously tested to assess basic flow characteristics and system pressure drop.[3] The core must be refurbished to incorporate additional instrumentation for measuring core block temperatures and to replace the existing graphite heater elements that have

undergone a significant amount of thermal cycling during previous checkout tests. Instrumentation will be positioned to provide extensive characterization of the core block temperature, both axially and radially, and to monitor coolant gas temperature in regions of interest. Details of the proposed instrumentation will be discussed in this Technical Memorandum (TM). More detailed characterization of core temperatures will allow implementation of a higher fidelity neutronics model that incorporates multiple, localized reactivity feedback coefficients as a function of various independent core temperature measurements. Additionally, investigation of deflection measurement techniques for application inside a pressure vessel has commenced and their potential applicability of these methods will be discussed.

2. SYSTEM MODEL: POINT REACTOR KINETICS

Reactor dynamics can be modeled using the point kinetics equations (PKEs), which can be derived from transport and diffusion theory.[4] The PKEs representation provides only an approximate model of the reactor; it does not provide a mechanism to describe neutron energy effects or structural details in a heterogeneous reactor. Because fast reactors are relatively small in size and do not contain any moderator to slow the neutrons to a lower energy, the PKEs are a good approximation for the dynamics in a fast reactor. In the absence of an external source and written in terms of reactor thermal power, the PKEs are given by

$$\frac{dP}{dt} = \frac{(\rho - \beta)}{\Lambda} P + \lambda_i C_i \tag{1}$$

and

$$\frac{dC_i}{dt} = \frac{\beta_i}{\Lambda} P - \lambda_i C_i \; , \tag{2}$$

where the reactivity, ρ, is given by

$$\rho = \frac{k-1}{k} \tag{3}$$

and k is the effective neutron multiplication factor. Reactivity is often expressed in units of dollars. The reactivity scale between zero and β, the total delayed neutron fraction, is divided into 100 cents, where 100 cents of reactivity are equal to 1 dollar. Hence, the reactivity expressed in units of dollars is given by ρ / β .

Studies of reactor dynamics generally recognize six distinct groups of delayed neutrons. Approximate solutions to the PKEs can be found using a smaller number of groups to represent the delayed neutron population. The dynamic model applied in the previous application of simulated reactivity feedback on the SAFE–100a included a simple dynamic model having one group of delayed neutrons, applying a weighted average decay constant and the total delayed neutron fraction. The one group decay constant (λ) is calculated as a weighted average of the six individual decay constants. A one-group representation simplified the computational model, speeding the real-time implementation of simulated reactivity feedback during test. However, to improve the fidelity of the neutronic model, a more detailed PKEs representation should be employed.

A complete six-group model, requiring seven ordinary differential equations, will be applied in DDG testing. The individual decay constants and delayed neutron fractions for a fast spectrum reactor,

as reported by Hetrick, are provided in Table 1.[4] To maintain real-time implementation of the neutronics model, with updates to the PKEs solution implemented on the order of 2 Hz, high-speed computing must be employed. Potential options for implementing real-time system control will be discussed in section 5.

Table 1. Delayed neutron properties for fast fission of ^{235}U.

Delayed Neutron Group	Decay Constant λ_i (s)$^{-1}$	Relative Yield β_i/β
1	0.0127	0.038
2	0.0317	0.213
3	0.115	0.188
4	0.311	0.407
5	1.4	0.128
6	3.87	0.026

Total decay constant, $\lambda = 0.0767$ s^{-1}
Total delayed neutron fraction, $\beta = 0.00642$

A simple model of a point reactor with feedback was applied in approximating the temperature reactivity feedback in the SAFE–100a. In that application, a single bulk reactivity feedback coefficient (α_T) was applied to the entire core. The feedback calculation was then made based on bulk core temperature changes that were determined by measuring multiple temperatures at the axial core centerline, and calculating the average core temperature using these data. In this simple case the total reactivity of the reactor core is given by equation (4) as:

$$\rho = \rho_o + \alpha_T \left(\Delta T \right) , \tag{4}$$

where α_T is the temperature coefficient of reactivity,

$$\alpha_T = \frac{d\rho}{dT} , \tag{5}$$

and ρ_o is the initial steady state reactivity before a transient is applied to the reactor power. In the previous application, α_T represented a bulk feedback coefficient, incorporating all reactivity feedback effects due to fuel and structural temperature changes, including Doppler broadened cross sections and thermal expansion effects. However, if highly precise temperature (and possibly deflection) measurements can be made, each of these individual effects on reactivity can be assessed separately in the feedback model. For example, equation (4) would be expanded to include several components of reactivity feedback as follows:

$$\rho = \rho_o + \rho_{dL} \left(dL(T) \right) + \alpha_{T,\text{fuel}} \left(\Delta T_{\text{fuel}} \right) + \alpha_{T,\text{block}} \left(\Delta T_{\text{block}} \right) + \alpha_{T,\text{reflector}} \left(\Delta T_{\text{reflector}} \right) + \cdots . \tag{6}$$

5

In equation (6), temperature feedback was broken into components based on the measured core dimensions and the current fuel, core block, and reflector temperatures. In nonnuclear testing, fuel temperature changes must be approximated from measured temperatures in the electric heating element or heater sheath, which is equivalent to the fuel-clad structure. Additionally, the nonnuclear test article may not incorporate a full reflector. In this case, the reflector temperature can be inferred from measured temperatures near the periphery of the core block and at the periphery of the pressure vessel in the case of a reactor cooled by a pumped fluid, as in the DDG.

One might choose to base reactivity feedback calculations solely on temperature measurements in various locations, or one might determine reactivity feedback from measured deflection in various regions of the core. Monte Carlo calculations can be performed to assess the reactivity worth of various core deflections that occur due to elevated temperature during core operation. The largest reactivity worth in a fast-spectrum reactor is expected to be due to fuel expansion with temperature, which can be further separated into radial and axial expansion; however, in the absence of an electric heater that closely mimics the dynamic characteristics of nuclear fuel, including thermal expansion, deflection-based reactivity feedback will likely need to be based on measured deflection of the core block, as was performed in SAFE–100 testing.[1] Options for measuring the deflection inside the DDG pressure vessel will be discussed in section 4.2.

3. TEST ARTICLE DESCRIPTION

The DDG is a gas cooled, UN-fueled, pin-type fast reactor designed to use helium-xenon (HeXe) gas flowing directly into a recuperated Brayton system to produce electricity for nuclear-electric propulsion.[5] The DDG, which consists of 37 fuel pins in a block matrix, is designed to operate at 32 kW thermal. This is a reduced power version of a full-scale design, similar to the SAFE-30 test series that preceded the SAFE–100 and 100a test series.[6] Each fuel pin is surrounded by an annular flow channel that provides direct heat removal by flowing gas. The DDG design was initially provided by Sandia National Laboratories but was transferred to Los Alamos National Laboratories for additional testing support. The DDG is constructed entirely of stainless steel. The core block is a 53.3-cm (21-in) long, 16.5-cm (6.5-in) (flat-to-flat) hexagonal, solid stainless steel block with a pattern of 37 gun-drilled 0.75-in-diameter holes through the length. A closeup of the core inlet region, with graphite electric heaters (thermal simulators) installed, is shown in figure 2.
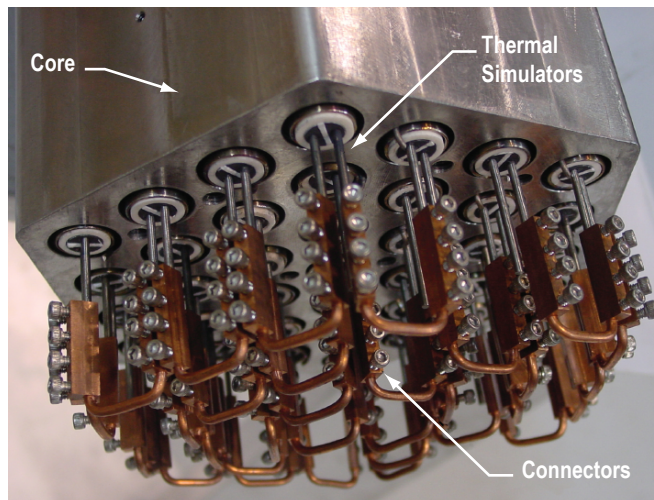

Figure 2. Core block inlet end with graphite heater elements installed.

The DDG was designed to operate at 2.4 MPa (350 psia) using an HeAr gas coolant with a core inlet temperature of 650 K, core exit temperature of 850 K, and bulk coolant flow of 0.1 kg/s. HeAr, which can duplicate the HeXe gas requirements, can be used in early tests to reduce the cost of the test program. Initial DDG testing was performed with nitrogen (N_2) gas to allow early system checkouts and verification of the test matrix for early problem identification, with gas-flow parameters selected based on a Reynolds number comparison. The test article is also plumbed to allow testing with any desired mixture of He and Ar. In the DDG design, the coolant gas enters the upper bonnet and is directed via a manifold to six 2.54-cm (1-in) inlet tubes located on the upper bonnet assembly, as shown in figures 3 and 4. The gas then flows down between the pressure vessel wall, called the downcomer region,
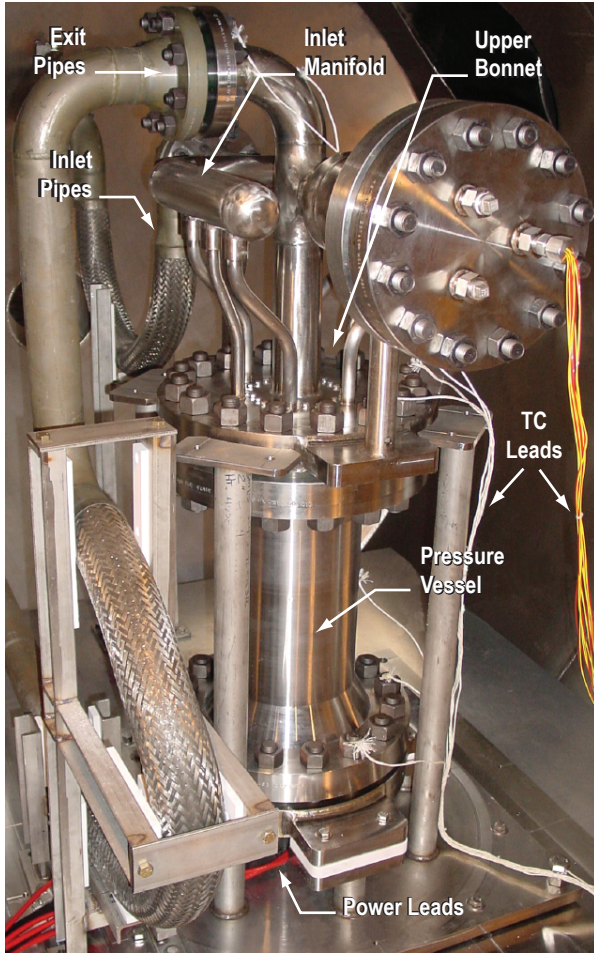
Figure 3. DDG test article installed in the vacuum chamber.
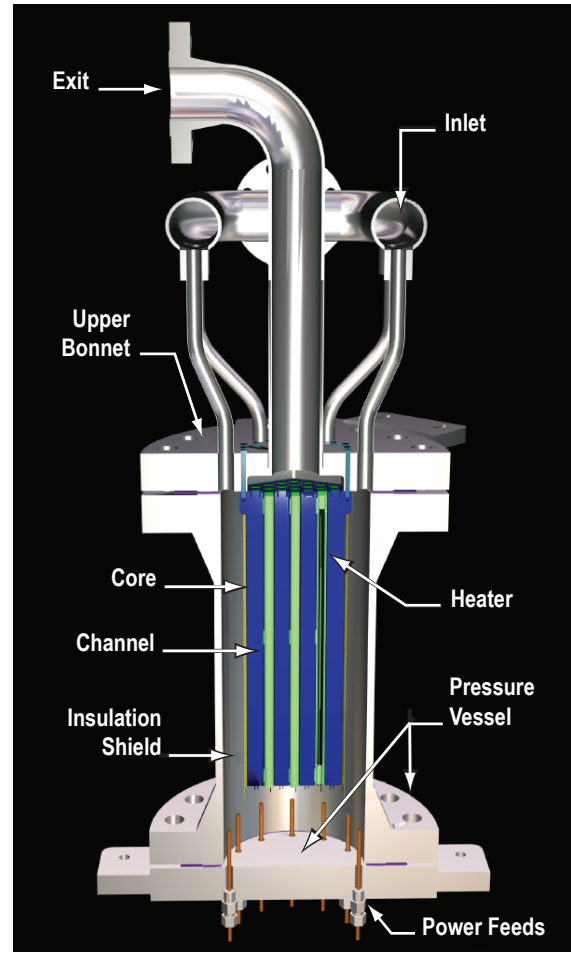
Figure 4. Graphical rendering of the DDG.

keeping the vessel wall at a constant lower temperature and providing gas insulation of the core. The insulation layer is constructed by including a metal shield between the core block and the pressure vessel wall, causing a stagnant gas layer to form between the core block and the metal shield. At the base of the pressure vessel, the gas collects in a plenum and is directed back up through 37 annular flow channels in the core. Flow parameters are selected such that the gas is heated ≈200 K through the core. Exit gas is then collected in an exit plenum where the flow is recombined and allowed to exit through the upper bonnet center exit pipe.

4. INSTRUMENTATION PLAN

Initial DDG checkout testing was performed with minimal instrumentation of the DDG test article. The primary intent of these initial tests was to verify core operation, assess gas-flow temperatures, and determine experimentally the core pressure drop to validate thermal hydraulics codes. A majority of the TCs were installed to measure gas-flow temperature in various regions. A few TCs were tack welded to the core block surface to obtain an approximate block temperature, but the temperature measurements from these TCs likely provided a combined block and flow temperature. Rather than being embedded in the core block, these TCs were mounted to the upper block surface where gas flow provided some cooling of the TC junction. No temperature measurements were made in the internal block region. During refurbishment of the DDG core, necessary to install new electric heaters for the next phase of testing, significant modifications will be made to the core instrumentation to provide the necessary data for implementation of simulated reactivity feedback in dynamic system testing.

4.1 Temperature Measurement

Various options for temperature measurement in the DDG core block and heater elements are currently being investigated. Ideally, temperature measurements would be made in the gas-flow regions within the core block, and between the electric heater and the sheath/fuel clad to obtain an estimate of fuel temperature. Gas-flow temperatures were measured in the initial DDG testing and will again be measured in planned tests. Additional type-K TCs will be positioned in key regions of interest to assess gas temperature: two in the gas blanket insulation region, two in the flowing gas downcomer region, two in the gas inlet plenum, and two in the gas outlet plenum. Additional TCs will be placed throughout the core block to fully characterize the block temperature both radially and axially. Methods of measuring the temperature near the heater element are also being investigated.

4.1.1 Core Block Temperature Measurements

A series of sheathed, type-K TCs will be installed throughout the DDG core block to fully characterize axial and radial temperature distribution. To minimize potential damage to the core block, machining of the block necessary for TC placement will be kept to a minimum. To characterize the axial temperature distribution, it is desirable to obtain temperature measurements along the core centerline and periphery at several axial locations. To accomplish this, the central heating element will be removed (reducing the number of heaters and flow channels to 36, representing a design configuration in which a central safety rod might be used) and will be replaced with an Inconel® sheathed axial profile probe. Manufactured by Omega, these probes can be purchased in the desired length and diameter, with the number and location of TCs located along that length also specified by the customer. The DDG core block is 52.7-cm (20.75-in) long and is equipped with 50.8-cm (20-in) heater elements. The bore holes in the core that accommodate a heater, sheath, and annular flow path are 1.9-cm (0.75-in) diameter. For DDG testing, a 51.4-cm (20.25-in), 1.7-cm (0.67-in) diameter probe will be employed with 10 TCs located at seven unique axial positions—2.54, 10.5, 18.4, 26.4, 34.3, 42.2, and 50.2 cm (1, 4.125, 7.25,

10.375, 13.5, 16.625, and 19.75 in). To ensure that measurements can be taken at these positions, even in the case of a failed TC, two independent TCs will be located at three different locations: 2.54, 26.4, and 50.2 cm (1, 10.375, and 19.75 in). A 1.3-cm (0.5-in) long metal plug installed in the central channel at the gas exit end of the core will prevent gas flow along the axial profile probe. Positioning the first and last TCs 2.54 cm (1 in) from either end of the core block ensures that they will be located in the heated region, accounting for the slightly shorter heating element (50.8-cm versus 52.7-cm core block). The axial centerline probe will be complemented by seven TCs located on the core periphery, embedded ≈0.64 cm (0.25 in) into the core block. The axial positions of these TCs are selected to correspond with the TC positions in the profile probe, as shown in figure 5.
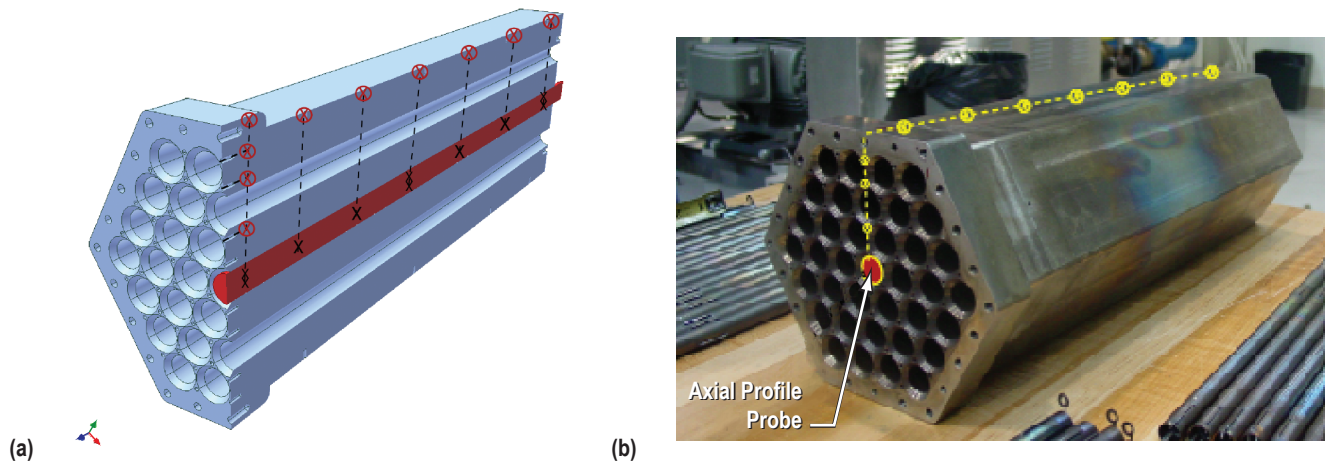

(a)

(b)

Axial Profile
Probe

Figure 5. (a) Graphical rendering and (b) hardware representation of axial TC placement in the DDG core block with the central element replaced by an axial profile probe; TC locations are denoted by small circles.

The radial temperature profile will be obtained by embedding TCs into the core block at both the inlet and outlet surfaces. The TC positions are selected to provide radial profiles of interest in two dimensions at each core surface. These TCs will be embedded ≈2.54 cm (1 in) into the block to ensure that they are located in the heated region as discussed above. Complete radial profiles at either end of the core block and complete measurement of the axial profiles along the centerline and the periphery will allow the radial temperature profile to be interpolated at any axial position. Proposed TC locations are superimposed on photos of the core block in figure 6. The proposed positions on the gas exit end of the core take advantage of existing mounting holes in the core block (originally intended for placement of flow orifice pieces) that are not currently being used. These holes will be bored to the desired 2.54-cm (1-in) depth for TC placement. Dashed lines in figure 6 show the approximate temperature profile obtained from surface TC measurements.
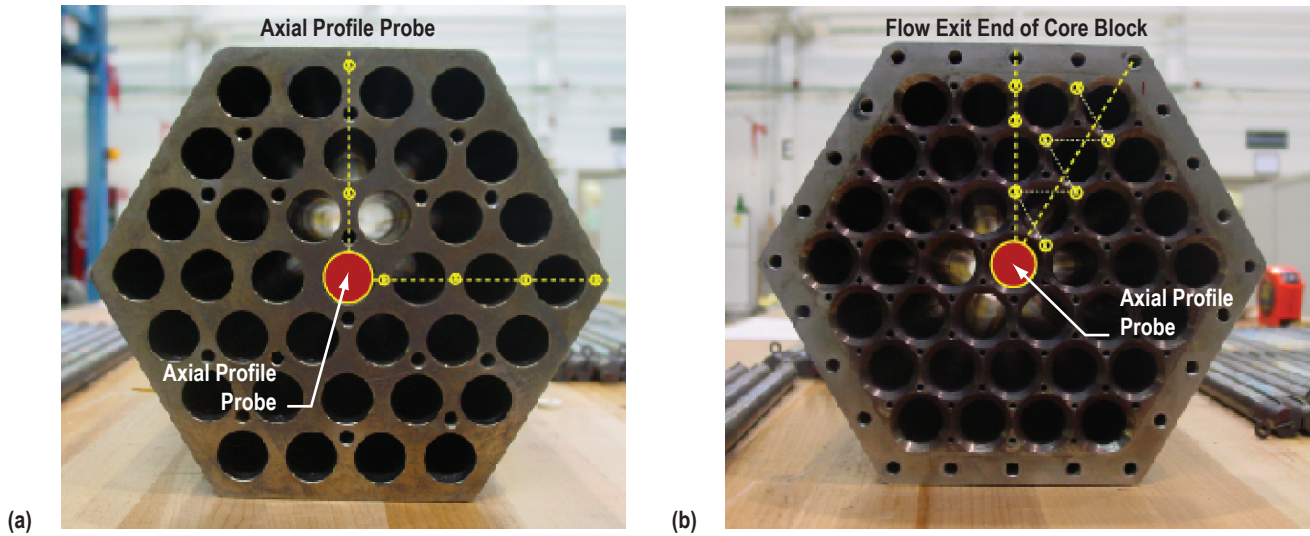
Figure 6. Radial TC placement on the (a) Flow entrance (heater end) and (b) flow exit ends of the DDG core block; the central element is replaced by an axial profile probe and TC locations are denoted by small circles.

4.1.2 Fuel Temperature Measurement

To implement detailed reactivity feedback, it is also desirable to measure temperature in the heater region to approximate the corresponding fuel temperature at a given power level, which requires the insertion of a temperature measurement device into the 0.7-cm (0.28 in) gap between the graphite heater element and the sheath structure, shown in figure 7; the gap is currently filled by an alumina space ring at three axial locations. This may be accomplished with very fine TCs embedded in the insulator rings on the heater element, or fiber optic probes might be inserted along the length to obtain a complete description of the temperature in this region at multiple axial positions.
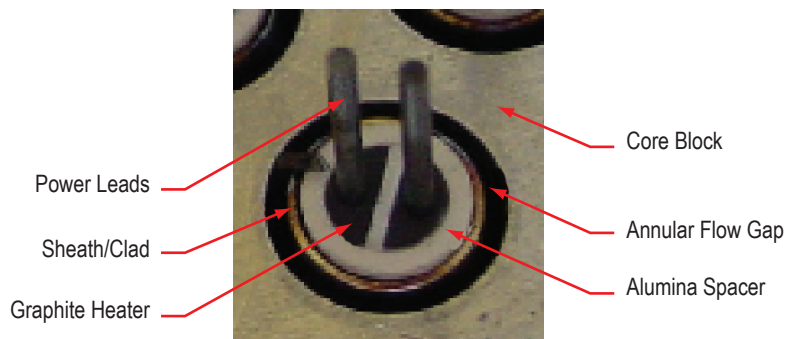

Figure 7. Heater element placement inside the DDG core block.

Fiber optic temperature probes developed by Luna Innovations, Inc. are constructed with Bragg gratings spaced evenly along the sensing length to obtain detailed temperature profiles; standard fiber optic design allows measurement of temperature at 1-cm (0.39-in) increments. These fiber optics currently have a temperature limitation of 1,273 °K for testing over extended times and may not survive over long test times at elevated temperatures in the DDG core. Luna fiber optic probes tested on the SAFE–100 demonstrated superior ability in generating three dimensional temperature profiles of the core.[7] Luna is currently working to extend the maximum operating temperature of the fiber optic sensors, which may qualify them for use as embedded temperature instrumentation in future advanced heater elements. Previous tests with Luna fiber optics were conducted by Luna, who brought the support hardware necessary to obtain and record data from the fiber optic probes to MSFC for temporary use. The EFF–TF is currently working to obtain an in-house capability to use fiber optic sensing techniques in future testing applications.

At present, standard TCs have been investigated to measure temperature along the heating element. Because TCs are relatively inexpensive and are available in a wide range of sizes and configurations, it was feasible to test a proposed configuration in a relatively short time frame. Six 0.254-mm (0.01-in) diameter, Inconel-sheathed type-K TCs with an ungrounded junction were procured to assess their applicability in DDG testing. Graphite heater elements used in the DDG testing are 0.985 cm (0.375 in) in diameter and are single ended (designed such that both inlet and outlet power leads are on a single end). These heater elements fit inside a 1.4-cm (0.55-in) diameter sheath, the outer diameter of which forms the annular flow path. The heater is separated from the sheath using three alumina spacer rings to prevent contact between the graphite element and the metal sheath. The junction end of a TC was bonded to the graphite element at each alumina ring using alumina cement to obtain three temperature measurements along each element, as shown in figure 8. During testing, several problems were noted with this configuration. Because the TC sheath is made of an electrically conductive material (Inconel), bonding the sheath to the heater in more than one location set up a parallel current path in the Inconel sheath. The current required to operate the heater element caused the TC sheath to vaporize and the 52 guage TC wires did not survive. Future investigation will consider alternate methods of embedding TCs within the heater elements to obtain approximate fuel temperature measurements; e.g., measurement of heater temperature that can be directly correlated to the expected fuel temperature at comparable conditions.
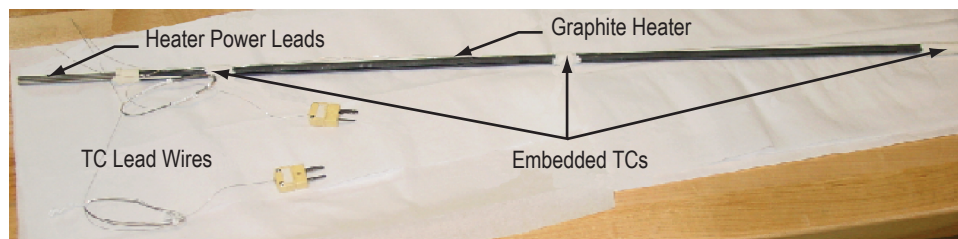

Figure 8. TC location on graphite heater element for preliminary testing.

4.2 Deflection Measurement

Reactivity feedback based on core deflection measurements was implemented in SAFE–100 hardware testing.[1] Note that tests discussed in section 1 were performed on the SAFE–100a, a 19-module partial array of the SAFE–100 design that utilizes Na-filled HPs and is coupled to a prototypic gas-flow HX. The SAFE–100 was a predecessor to the SAFE–100a. The SAFE–100, designed to provide 100 kW power, includes 61 modules, each containing three fuel tubes and one HP. In the test article, a total of 183 graphite resistance heaters were used to simulate the heat of nuclear fission. However, the SAFE–100 test article had no mechanism for heat removal from the core; hollow stainless steel tubes were used to represent the HPs in each module. As a result, this test article was used to simulate the operation of a fission system in the absence of cooling; this condition is similar to the operation of a HP reactor during the start-up period prior to complete thaw of the HP working fluid and initialization of the HXs. Deflection tests were performed on the 316 stainless steel (SS316) SAFE–100 core, manufactured according to the SAFE–100 core fabrication drawings.

Because the SAFE–100 did not require a pressure vessel, visual access to the core was maintained. In this case, deflection could be measured using high-resolution photography. Mounted outside the vacuum chamber, imagery from a 6.3 mega-pixel high-resolution camera, composed of a charge-coupled device (CCD) and a camera lens, was used to assess core deflection as a function of temperature by scanning multiple cross sections along the axial dimension of the core (fig. 9). The SAFE–100 was located on an immobile stand inside the chamber, and the CCD imaging system had a clear view of the core through a fused silica viewing port.
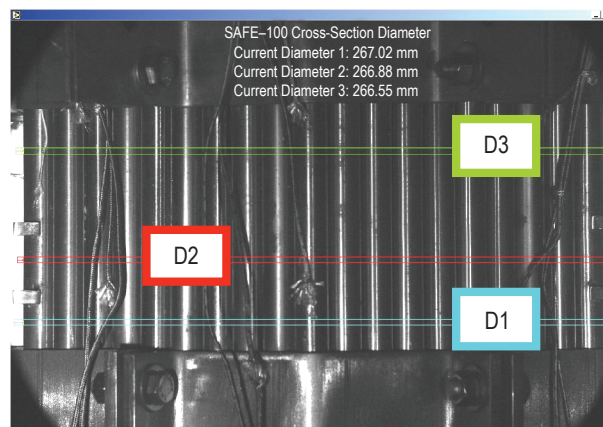
Figure 9. Screen shot taken during SAFE–100 testing identifying
three axial locations for core width measurement.

Deflection measurement becomes increasingly complex when visual access is not readily available. Because the DDG must be tested inside a pressure vessel, novel deflection measurement techniques must be investigated. Displacement can be measured using an optical proximity sensor; e.g. a laser range finder, a differential variable reluctance transducer (DVRT), or a noncontact inductance proximity sensor. Each of these was evaluated for its applicability in DDG testing. The next stage of DDG testing will

be performed at ≈0.34 MPa (50 psi) to accommodate a Brayton energy conversion system that may be incorporated with the DDG hardware. This reduced pressure condition somewhat relaxes the requirements for a deflection measurement system, but the gas temperature will be approximately the same as in previous testing.

Initial investigations indicate that optical proximity sensors or laser range finders may not be reliable methods of deflection measurement. In this application, the sensor would be directed at the external core block surface. This would require a window to be installed in the DDG pressure vessel, and it is difficult to find ports with viewing windows rated for the experimental pressure and temperature conditions (in the downcomer region, the inlet gas flow is ≈450 K). Additionally, these instruments are dependent on the emissivity of the surface being investigated. As the core surface temperature increases, the emissivity of the stainless steel block changes such that the accuracy of the sensor over time can be compromised.

DVRTs were previously investigated for application to the SAFE–100 and–100a test articles. A DVRT uses a plunger that is in contact with the core surface. Deflection is then determined by measuring differential reluctance between magnetically shielded DVRT coils. Unfortunately, very few of the commercially available units are rated for high-temperature operation (>773 K). Although the sensor would not be in direct contact with the hot core block, the plunger conducts heat to the sensor and can cause the operating temperature to be exceeded.

Eliminating direct contact with the hot core block surface reduces the temperature that will be seen by a sensor housing. This can be accomplished using a noncontact inductance proximity sensor. These devices are commercially available for operation at pressure and at elevated temperatures. RDP Electrosense, Inc. manufactures high-temperature, noncontact transducers that employ an inductive proximity position sensor principle and will operate with any ferritic material. The output of the displacement transducer varies as the gap between the front face of the transducer and the target changes. These sensors have electron beam-welded joints and are rated for operation from full vacuum up to 20 MPa (2,900 psi) and up to 873 K. The RDP sensor can be purchased with a measurement range of up to 6 mm, with a quoted linearity of ±0.05 percent of full scale. Sensor model PY256C has been ordered to determine potential applicability in DDG testing. The sensor is currently being retrofitted to place a pressure feedthrough on the signal cable that will allow it to be installed through the DDG spool. The basic configuration is shown in figure 10. The sensor head itself is 4.8-cm (1.9-in) long with a maximum diameter of 2.8 cm (1.1 in), making it a tight fit between the core and the pressure vessel. The unit must be calibrated for operation in the desired environment prior to implementation, somewhat complicating its use. Initial calibration and testing will commence after the modified unit has been received and prior to integration in the DDG.
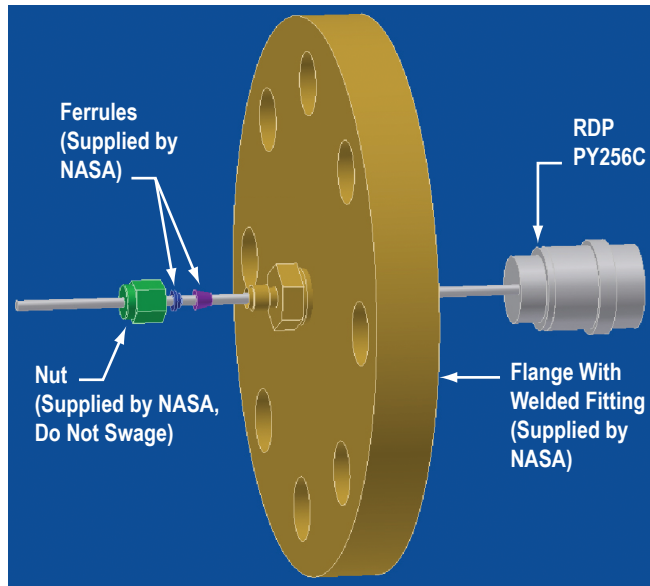
Figure 10. Configuration of the nocontact inductance proximity sensor for the measurement of core deflection during testing. The flange will be installed in the wall of the DDG pressure vessel, and the face of the RDP PY256C sensor will be directed toward the core block.

5. CONTROL METHODOLOGY: IMPLEMENTATION

Specialized LabVIEW® programs have been developed at the EFF–TF to implement all aspects of system operation. One visual interface provides power supply control while a second monitors core temperatures and controls the gas supply to remove heat from the core (either for the HX in the SAFE–100a or the direct gas flow through the DDG). To implement reactivity feedback control, the LabVIEW control program additionally implements a solution to the PKEs in order to govern core power response to the transient.

In SAFE–100a testing, which implemented the PKEs with one group of delayed neutrons, the neutronic model included only two differential equations (eqs. (1) and (2)). The simplicity of this model allowed the solution to the system of equations to be precalculated and programmed into LabVIEW in algebraic form, minimizing the computation time required by the LabVIEW data acquisition and control system. The solutions to the PKEs were then implemented in real time at each iteration of the control loop. All TCs installed in the test article were scanned at a rate of 5 Hz (approximately once every 200 ms). The power supply controller set points were updated at a rate of 1 Hz. Taking into consideration the time required to scan the TCs and depending on how well the scanning rate and the set point update rates were synchronized, the total lag between taking the temperature measurement and updating the controller set point varied between approximately 200 and 900 ms. Since there were multiple computers in the control loop, the total end-to-end lag would drift at a rate dependent on how well the clocks of each system matched. Quantitative measurements of the lag and drift were not made. It was assumed that the time constants of the physical processes were much greater than 900 ms in the tested system. Future modifications to the software architecture can be made to constrain the lag to a smaller fixed value with a small amount of jitter. With hardware changes even greater improvement can be achieved.

The basic control methodology that was applied in previous applications of dynamic testing is summarized in the schematic in figure 11. The system can basically be divided into three parts: (1) Test hardware, (2) LabVIEW data acquisition system, and (3) LabVIEW power control system. In this representation the test hardware consists of the core, instrumentation, and stand-alone power supplies. The test is controlled with two computer systems, both using customized programs built in LabVIEW. The LabVIEW data acquisition system collects data from all instrumentation and broadcasts that data over a local ethernet. The second system, the power control system, reads data broadcast by the data acquisition system, computes a new power level from the PKEs solution, and updates the set points used to control the power supplies.
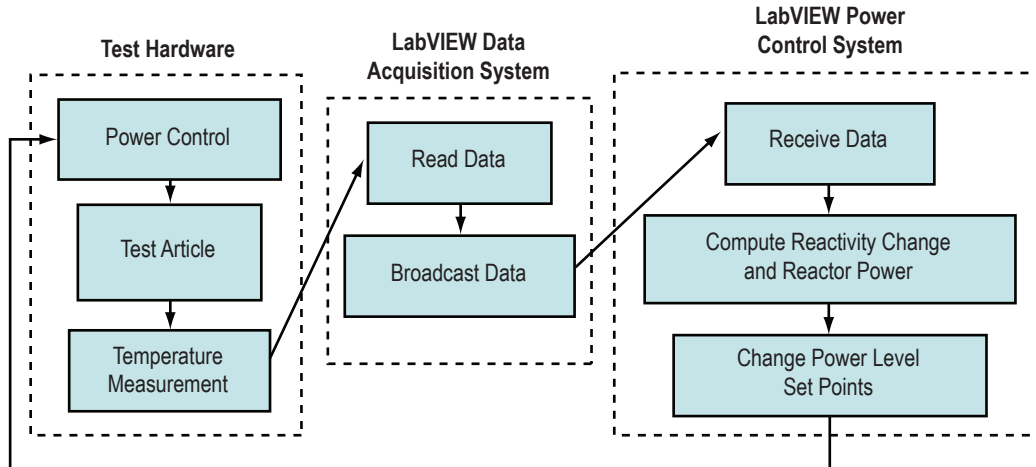
Figure 11. Schematic diagram of data flow for the SAFE–100a test system.

DDG testing will require increased computation time to solve a system of seven differential equations at each iteration of the control loop, due to the incorporation of six delayed neutron groups in the neutronic model. To accomplish this without impacting the control time, investigation has been initiated to determine ways in which the computational efficacy can be improved. Potential options for dynamic system control are summarized in table 2. Currently, the most promising arrangement appears to be the development of the neutronics model in a MATLAB® Simulink® code that can be operated on a separate computer that interfaces back to the governing LabVIEW data acquisition and control code. MATLAB Simulink utilizes a graphical, time-based differential equation solver. This arrangement requires that the dynamic model computer run xPC Target, an additional MATLAB product. The control computer can then communicate with the model computer, sending updated data to the Simulink model at specified time steps, which then returns the new power solution to the PKEs for application to the system. Both UDP communications and shared memory are being investigated as potential communication options between the target and control PCs.

Table 2. Software and hardware configurations for various data acquisition and control systems.

	Data Acquisition	Dynamic Model	Power Control	Description
1	LabVIEW—acquisition computer	LabVIEW—power control computer	LabVIEW—power control computer	SAFE–100a configuration. Dynamic model contains limited fidelity.
2	LabVIEW—acquisition computer	Simulink/LabVIEW interface toolkit-power control computer	LabVIEW—power control computer	Simulation Interface Toolkit for LabVIEW is required. Model is executed on same PC as LabVIEW.
3	LabVIEW—acquisition computer	Simulink/xPC target (UDP)—dynamic model computer	LabVIEW—power control computer	A separate PC running xPC target executes the model. Data are transferred between model and LabVIEW via UDP communication.
4	LabVIEW—acquisition computer	Simulink/xPC target (shared memory)—dynamic model computer	LabVIEW—power control computer	A separate PC running xPC target executes the model. Data are transferred via shared memory boards.

5.1 Execution of Dynamic Model Within LabVIEW

The first configuration listed in table 2 is the same as that described for the SAFE–100a test setup. Based on a change in temperature, which results in a change in the reactivity in a reactor, LabVIEW is used to compute a new solution to the PKEs, which is then translated to a new set of reactor power level setpoints over the projected time period. Although this method could be readily implemented on the DDG system, it becomes less desirable compared to other options that incorporate Simulink as the fidelity of the neutronic model is improved, increasing the computation time necessary at each application of the control loop.

5.2 Execution of Dynamic Model Within Simulink on LabVIEW PC

A Simulink model may be executed on the same PC as a LabVIEW program through the use of the Simulation Interface Toolkit produced by National Instruments. This toolkit allows for communication between a LabVIEW program and a Simulink model. To assess the benefits and limitations of this configuration, further work needs to be performed. Preliminary work has shown that, as configured, the toolkit allows for limited interaction between a Simulink model and LabVIEW program. LabVIEW Real Time software may be required to allow for increased functionality between the LabVIEW program and Simulink model. Although this configuration may require the least amount of hardware changes to the system, the added complexity to the LabVIEW program required to accommodate a Simulink interface may offset the added complexity of new hardware required in the remaining configuration options.

5.3 Execution of Dynamic Model on a Target PC with User Datagram Protocol Communications

5.3.1 xPC Target

To remove the computational burden of executing a Simulink model on the same PC as a LabVIEW program, xPC Target may be used to execute the Simulink model on a standalone PC. A boot disk produced by the xPC Target loads the xPC Target application on the target PC at bootup. With TCP/IP communication over an ethernet, the Simulink model may then be downloaded to the target PC. This may be accomplished several ways. If the model has already been built and compiled, LabVIEW may be used to communicate with the target PC through the use of application interface (API) drivers provided by MATLAB. Figure 12 shows the process used to build and deploy a model with xPC Target.

Figure 12. xPC Target model development process.

5.3.2 User Datagram Protocol Communication

Once the model has been downloaded to the target PC, it is ready to be used in the system. To interact with the rest of the test system, the model must be capable of receiving reactivity information, then sending the power computed from a solution to the PKEs. One possible method of communication between the model and target PCs is the UDP communication protocol. The SAFE–100a test system used this protocol to distribute data over the local ethernet.

To test the ability of the Simulink model to interact with the LabVIEW application via UDP communication, a LabVIEW application and Simulink model were created. The LabVIEW model created and sent the value of a sinusoidal signal once every 250 ms. The Simulink model was configured with a fixed step size of 250 ms. At each time step, the model read the most recent data from the communications port and then sent the data back to the LabVIEW model, where LabVIEW then read the data and displayed it. Testing indicated that synchronization of the LabVIEW software and the Simulink model was difficult in this configuration. Both the LabVIEW and Simulink systems were operating at a sample rate of 250 ms. Depending on when the Simulink model was started relative to the LabVIEW application, data received by the LabVIEW application could lag behind the sent data by as much as 250 ms. If this lag could be guaranteed, UDP communications might have been an acceptable method; however, if the LabVIEW application speeds up or slows down relative to the Simulink model (this is possible when windows are opened or closed on the LabVIEW PC), the lag between sent and received data could temporarily increase. Figure 13 shows data received by the LabVIEW application and the number of time steps between the sent and received data. This variable time lag between sent and received data could yield incorrect results from the dynamic model.
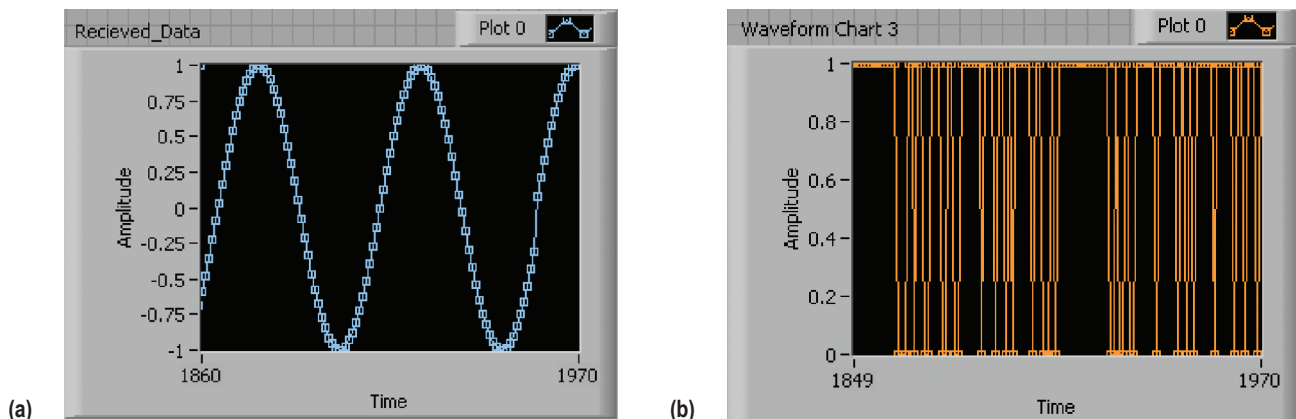

Figure 13. (a) Data received by LabVIEW and (b) time-step delay between sent and received data.

One method that could be used to mitigate the variability of the time lag between sent and received data would be to decrease the time step size of the Simulink model. With this method, sent data would be received sooner, then resent. This solution increases the required computational power in the target PC and, if time-dependent equations are used in the Simulink model, care must be used to ensure that the equations are solved over the correct time interval. Another avenue could be to use the

data to drive the model. If Simulink provides programmatic hooks for controlling when a model step is executed, the execution of each model step could be initiated whenever new data is received. In other words, the model could be driven by the data, and the variability of the time lag would be eliminated. This possibility still needs to be investigated.

5.4 Execution of Dynamic Model on a Target PC with Shared Memory

To ensure better synchronization of data between the Simulink model and LabVIEW application, the use of shared memory cards was evaluated. A VMIC 5565 shared memory board was installed on the PCI bus of both the host and target PCs. The shared memory boards transfer data by writing data to a specified partition on all boards in a network when data is written to a single board; therefore, when data is available on a single memory board, it is then instantaneously available on all the memory boards in the system. The boards are connected with fiber optic cable and allow for high data transfer rates. A second feature of the shared memory boards that helps with data synchronization is that the boards are capable of sending and receiving hardware interrupts. When using xPC Target, a Simulink model executes in real time. The use of hardware interrupts allows for an external signal to be used to dictate when the model should execute its next time step. Therefore, the Simulink model may be incremented by a single time step each time the LabVIEW application increases by a time step by sending an interrupt from the LabVIEW PC. With the neutronic models tested to date, the result at each time step was computed within approximately $1{\times}10^{-4}$ seconds. These data were then available to the LabVIEW application fractions of a second later. With this implementation, real-time execution of the dynamic model may be achieved—relative to the base system time scale of $\approx$200 ms.

Similar to the test performed with UDP communication, shared memory boards were used to send data from LabVIEW, read data with the Simulink model, and then send data back to LabVIEW. Through the use of network interrupts, a negligible time lag was found between the sent and received data in LabVIEW. Due to the high reliability of data transfer achieved with this method, this configuration is preferred to the others presented above. Additionally, the use of a separate PC for the execution of the dynamic model increases available computational capacity and allows for the implementation of larger, more complex dynamic models in the future.

5.5 Dynamic Model System Implementation

An implementation of the coupled LabVIEW-Simulink system was built to demonstrate the feasibility of implementing the improved neutronics model on a target PC. The test system was built with the shared memory configuration described in section 5.4. Although shared memory was used as the data transfer mechanism between the LabVIEW and Simulink systems, an ethernet connection was necessary between the two systems to allow for download and control of the model on the target PC.

A simple Simulink model was built to simulate the behavior of both the reactor kinetics and the thermal system that would normally be coupled to the electrically heated test system. Figure 14 shows the Simulink block diagram of the model. The first three blocks in the data path, shown in the model, ("5565 read," "5565 unpack," and "change endianess") read data from the shared memory board and prepare the data for Simulink calculations. The value of reactivity, based on the current core temperature, read from the shared memory board is then sent to the reactor power subsystem, which contains the

point kinetics representation of the reactor dynamics. The new power level calculated from the PKEs solution at that time step is then prepared and written to the shared memory board. The reactor power is also used to compute a new structural temperature with the core thermal model subsystem. This temperature is also written to the shared memory.
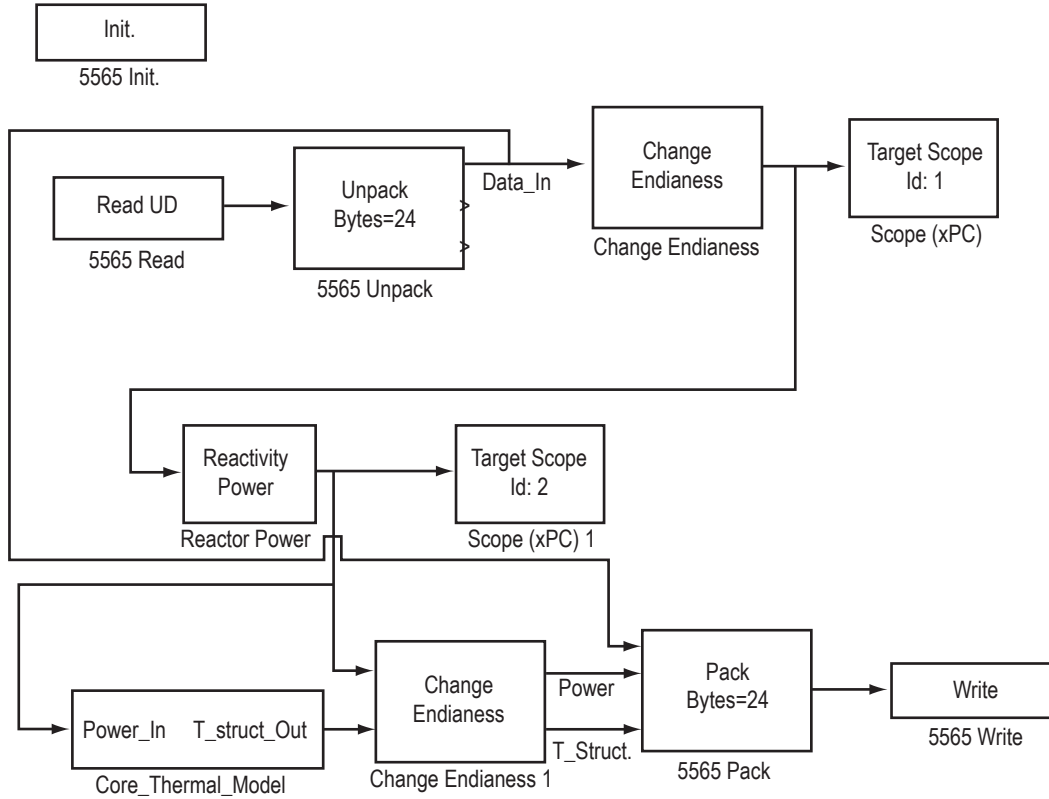

Figure 14. Simulink block diagram of the test dynamic model.

The core thermal model subsystem, shown in figure 15, was created to allow for a demonstration of reactivity temperature feedback effects. The thermal model consists of two energy balances. The first energy balance is for the structure of the core and may be represented analytically (eq. (7)):

$$T_{\text{struct}} = \frac{1}{M_{\text{struct}} \cdot C_{p,\text{struct}}} \cdot \int P_{Rx} - h_c \cdot A \cdot \left(T_{\text{struct}} - T_{\text{coolant,avg}} \right) \cdot \tag{7}$$
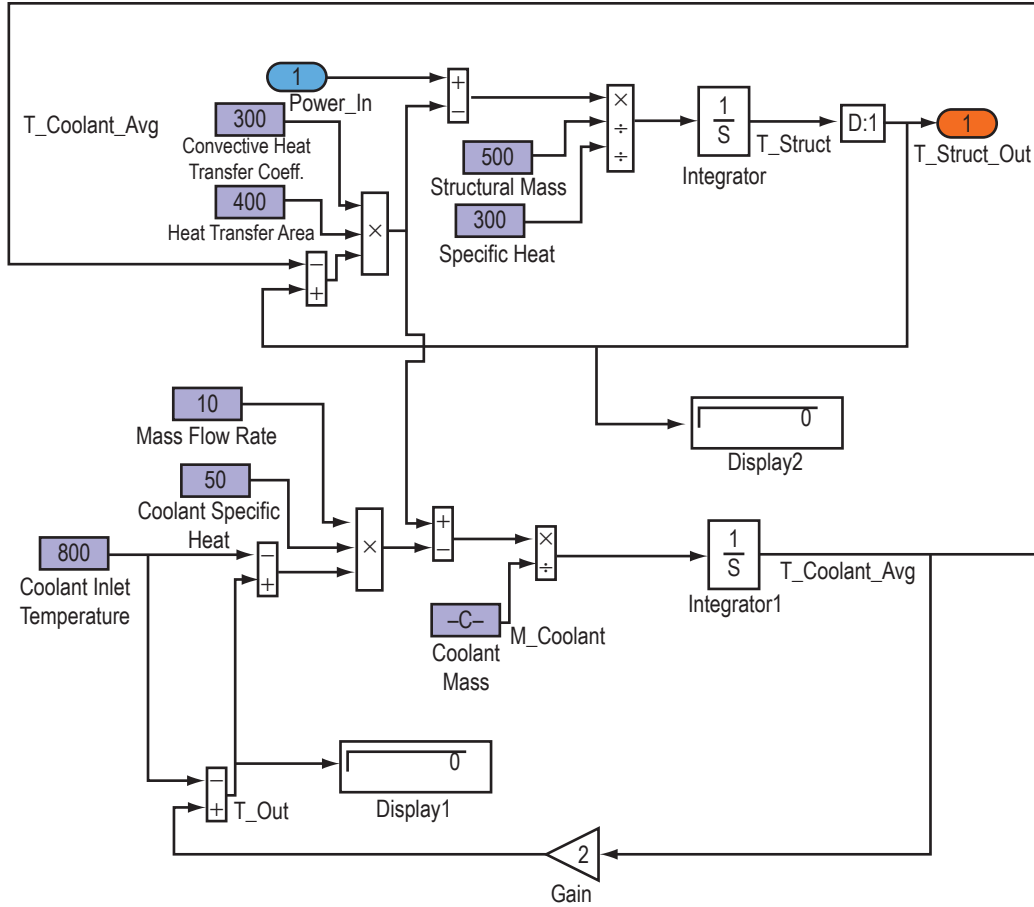
Figure 15. Simulink block diagram for the core thermal model.

Dummy values for the coolant and structural masses and other material properties were used in the test dynamic model. The energy balance of the coolant inside the core was computed using the relationship in equation (8):

$$T_{\text{coolant,avg}} = \frac{1}{M_{\text{coolant}} \cdot C_p} \cdot \int h_c \cdot A \cdot \left(T_{\text{struct}} - T_{\text{coolant,avg}}\right) - \dot{m} \cdot C_p \left(T_{\text{out}} - T_{\text{in}}\right) \; . \tag{8}$$

A simple LabVIEW application was built to test the functionality of the shared memory interface between the LabVIEW and target PCs. The LabVIEW application functions by reading temperature output from the thermal model then computing and sending a new value for the reactivity based on the new core temperature. The output of the model is then read and displayed by the LabVIEW application. Figure 16 shows the user interface to this program. The reactivity, power, and temperature are displayed on the waveform charts. The control labeled Inserted_Reactivity allows for the addition or removal of reactivity from the system; e.g., simulating a reactor control maneuver. For simulation purposes, the timed

loops in this application are set to run once every 25 ms, causing the Simulink model to run at ten times real time. The system appeared to behave as expected. The plots show a positive reactivity insertion followed by a negative reactivity insertion.

Figure 16. LabVIEW application: VMIC test.

The rate at which the power may be accurately updated depends on the speed at which data is made available. In the current test system, TC data is available at 5 Hz. The test system with reactivity feedback was simulated in Simulink at various data rates to demonstrate the model performance when the sample rate differs from the data rate. Figures 17–19 show the simulated response of the system to a reactivity insertion at $t = 100$ s. The model was run at a rate of 100 Hz. However, the reactivity feedback was sampled at various slower sample rates to demonstrate the effect of running the model faster than the data was being updated. Figure 17 shows the reactivity as a function of time. The black line shows the model response when the data rate is the same as the model speed (F_s=0.1s). In the simulation, temperature rises soon after the reactivity insertion, causing a drop in reactivity soon after the initial increase. When the data sample rate (F_s) is slower than the model sample rate, the model will compute the response using the last known value of reactivity. This causes the stepped shape of the curves in figure 17. When the model computes the time-dependent power response based on this constant

reactivity, an exponential increase is seen, causing the divergence between the black line and other lines at $t = 100$ s in figure 18. Although running the model at a faster sample rate than the data rate allows for a higher resolution time-dependent power function, there may actually be more error in the controlled power relative to the real, continuous system than if the power was held at a constant value until new temperature data were available.
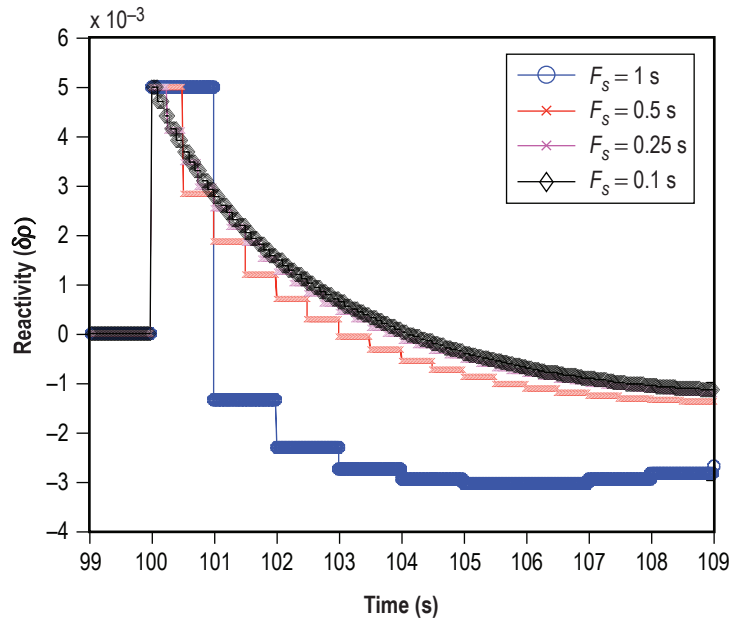

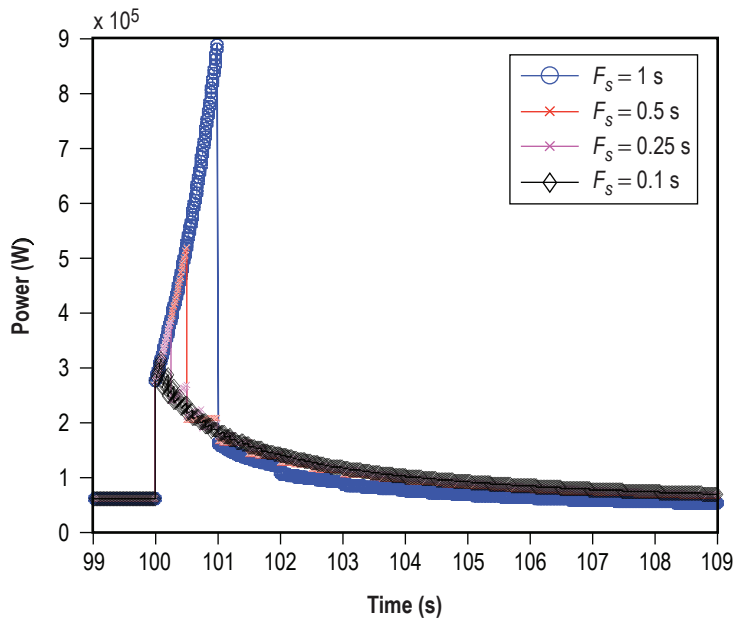Figure 17. Simulated reactivity response to a reactivity insertion at various data rates.

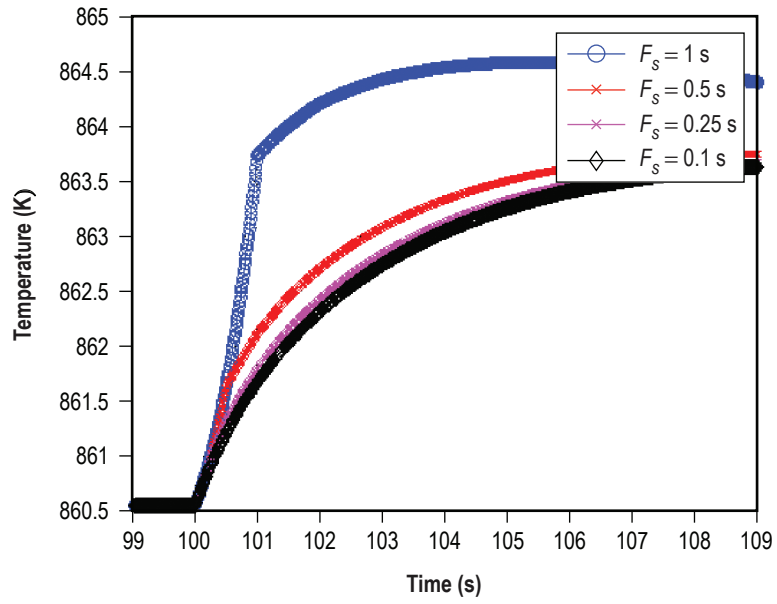Figure 18. Simulated power response to a reactivity insertion at various data rates.

Figure 19. Simulated temperature response to a reactivity insertion at various data rates.

5.6 Selection of a Computing Environment for Dynamic Testing

As previously discussed, several methods can be adopted to improve the dynamic testing capability at the EFF–TF. After evaluating several potential configurations, separate model and control computers were selected over a configuration in which Simulink and LabVIEW would be run on the same PC. At present, the most desirable option that can be readily implemented will incorporate Simulink and xPC Target software and will use shared memory boards for data transfer between PCs, providing the simplest and most reliable solution. This configuration minimizes complexity within the LabVIEW program that would be required to directly interface with Simulink on a single PC. Additionally, using a single processor places a fundamental limit on the complexity that can be added to the Simulink model while maintaining reasonable calculation rates; hence, the selected configuration offers the greatest capacity for future model expansions. The capability of updating data acquisition and control information at 100-ms time steps is currently being investigated.

6. CONCLUSIONS

Integrated system tests with simulated reactivity feedback on the SAFE–100a demonstrated the potential benefits to system operation with simulated neutronic response based on measured system conditions. By simulating dynamic system response, a better understanding can be gained with respect to system integration issues, system response times and response characteristics, and overall system design potentially allowing for design improvements prior to large fiscal and manpower investments into a nuclear test program. Plans are underway to implement similar test methodology on the DDG at the EFF–TF. This implementation will incorporate higher fidelity neutronic models and will utilize more detailed measurements of the system state, as described in this TM. Necessary system modifications could be completed within ≈2 mo with dynamic tests commencing shortly thereafter.

REFERENCES

1. Bragg-Sitton, S.M.; and Forsbacka, M.: "Application of a Virtual Reactivity Feedback Control Loop in Nonnuclear Testing of a Fast Spectrum Reactor," Proceedings of the *International Congress on Advanced Nuclear Power Plants* (*ICAPP–2004*), American Nuclear Society Order No. 700306, Pittsburgh, PA, pp. 2259–2268, 2004.

2. Bragg-Sitton, S.M.: "Heat Pipe Reactor Dynamic Response Tests: SAFE–100a Reactor Core Prototype," Proceedings of the *Space Nuclear Conference* (*SNC–2005*), American Nuclear Society, San Diego, CA, pp. 781–789, 2005.

3. Godfroy, T.J.; Kapernick, R.; and Bragg-Sitton, S.M.: "Thermally Simulated 32 kW Direct-Drive Gas-Cooled Reactor: Design, Assembly and Test, " Proceedings of *Space Technology and Applications International Forum* (*STAIF–2004*), M. El-Genk (ed.), AIP Conference Proceedings 699, New York, pp. 757–763, 2004.

4. Hetrick, D.L.: *Dynamics of Nuclear Reactors*, The University of Chicago Press, Chicago, IL, 1971.

5. Wright, S.A.; and Lipinski, R.J.: "Pin-Type Gas Cooled Reactor for Nuclear Electric Propulsion," in proceedings of *Space Technology and Applications International Forum* (*STAIF–2003*), M. El-Genk (ed.), AIP Conference Proceedings 654, New York, pp. 408–419, 2003.

6. VanDyke, M.K.; Houts, M.G.; Pedersen, K.; et al.: "Phase I Space Fission Propulsion System Testing and Development Progress, " in proceedings of *Space Technology and Applications International Forum (STAIF–2001)*, M. El-Genk (ed.), AIP Conference Proceedings 552, New York, pp. 837–842, 2001.

7. Stinson-Bagby, K.L.; and Fielder, R.S.: "Fiber Bragg Gratings for High-Temperature Thermal Characterization," in proceedings of the *International Congress on Advanced Nuclear Power Plants* (*ICAPP–2004*), American Nuclear Society Order No. 700306, Pittsburgh, PA, pp. 2288–2294, 2004.

REPORT DOCUMENTATION PAGE

1. AGENCY USE ONLY *(Leave Blank)*	2. REPORT DATE June 2007	3. REPORT TYPE AND DATES COVERED Technical Memorandum

4. TITLE AND SUBTITLE

Application of Simulated Reactivity Feedback in Nonnuclear Testing of a Direct-Drive Gas-Cooled Reactor

5. FUNDING NUMBERS

6. AUTHORS

S.M. Bragg-Sitton and K.L. Webster

7. PERFORMING ORGANIZATION NAME(S) AND ADDRESS(ES)

George C. Marshall Space Flight Center
Marshall Space Flight Center, AL 35812

8. PERFORMING ORGANIZATION REPORT NUMBER

M–1188

9. SPONSORING/MONITORING AGENCY NAME(S) AND ADDRESS(ES)

National Aeronautics and Space Administration
Washington, DC 20546–0001

10. SPONSORING/MONITORING AGENCY REPORT NUMBER

NASA/TM—2007–214959

11. SUPPLEMENTARY NOTES

Prepared by the Propulsion Systems Department, Engineering Directorate

12a. DISTRIBUTION/AVAILABILITY STATEMENT

Unclassified-Unlimited
Subject Category 31
Availability: NASA CASI 301–621–0390

12b. DISTRIBUTION CODE

13. ABSTRACT *(Maximum 200 words)*

Nonnuclear testing can be a valuable tool in the development of an in-space nuclear power or propulsion system. In a nonnuclear test facility, electric heaters are used to simulate heat from nuclear fuel. Standard testing allows one to fully assess thermal, heat transfer, and stress related attributes of a given system but fails to demonstrate the dynamic response that would be present in an integrated, fueled reactor system. The integration of thermal hydraulic hardware tests with simulated neutronic response provides a bridge between electrically heated testing and full nuclear testing. By implementing a neutronic response model to simulate the dynamic response that would be expected in a fueled reactor system, one can better understand system integration issues, characterize integrated system response times and response and response characteristics, and assess potential design improvements with a relatively small fiscal investment. Initial system dynamic response testing was demonstrated on the integrated SAFE–100a heat pipe cooled, electrically heated reactor and heat exchanger hardware. This Technical Memorandum discusses the status of the planned dynamic test methodology for implementation in the direct-drive gas-cooled reactor testing and assesses the additional instrumentation needed to implement high-fidelity dynamic testing.

14. SUBJECT TERMS

nonnuclear testing, reactivity feedback, dynamic simulation

15. NUMBER OF PAGES

40

16. PRICE CODE

17. SECURITY CLASSIFICATION OF REPORT Unclassified	18. SECURITY CLASSIFICATION OF THIS PAGE Unclassified	19. SECURITY CLASSIFICATION OF ABSTRACT Unclassified	20. LIMITATION OF ABSTRACT Unlimited

National Aeronautics and
Space Administration
IS20
George C. Marshall Space Flight Center
Marshall Space Flight Center, Alabama
35812